Seismic Fragility Curves for Multi-Span Concrete Bridges

다경간 콘크리트 교량의 지진 취약도

김 상 훈*
Kim, Sang Hoon

국문요약

다수의 지점 위에 놓인 교량의 경우, 지진으로 인한 지반운동은 교량길이에 따른 거리에 걸쳐 지점마다 현저하게 다를 수 있다. 본 연구는 이러한 공간적 특성을 고려하기 위하여 지점마다 다른 진폭과 위상 그리고 주파수 성분을 갖도록 지반운동 시간이력곡선을 생성하였고, Monte Carlo 해석기법을 사용하여 생성된 지반운동 하에서 교량의 비선형 동적거동을 고찰하였으며 두개의 실제 교량에 대한 취약도 해석을 수행하였다. 공간적 특성이 지진반응에 미치는 영향을 고려하여 교량교각의 연성도에 대한 취약도 곡선을 개발하였고, 동일지진 하에서의 취약도 곡선과 비교 검토하였다. 본 연구는 동일 지반운동을 사용하여 교량해석을 수행하는 경우 교각의 요구 연성계수가 상이 지반운동을 사용하는 경우보다 저평가 될 수 있다는 것을 입증하였다. 지진취약도 곡선은 지반운동의 강도를 표시하는 PGA, PGV, SA, SV와 SI의 함수로 나타내어졌다. 본 연구는 최초로 공간적 특성을 반영한 지반운동 하에서의 지진취약도 곡선을 개발하였으며, 다경간 교량의 내진설계시 시방서에 그 영향을 고려하기 위한 설계지침의 근거를 제공할 것이다.

주요어 : 취약도 곡선, 콘크리트교량, 비선형 동적해석, 내진, 연성계수

ABSTRACT

Seismic ground motion can vary significantly over distances comparable to the length of a majority of highway bridges on multiple supports. This paper presents results of fragility analysis of two actual highway bridges under ground motion with spatial variation. Ground motion time histories are artificially generated with different amplitudes, phases, as well as frequency contents at different support locations. Monte Carlo simulation is performed to study dynamic responses of the bridges under these ground motions. The effect of spatial variation on the seismic response is systematically examined and the resulting fragility curves are compared with those under identical support ground motion. This study shows that ductility demands for the bridge columns can be underestimated if the bridge is analyzed using identical support ground motions rather than differential support ground motions. Fragility curves are developed as functions of different measures of ground motion intensity including peak ground acceleration(PGA), peak ground velocity(PGV), spectral acceleration(SA), spectral velocity(SV) and spectral intensity(SI). This study represents a first attempt to develop fragility curves under spatially varying ground motion and provides information useful for improvement of the current seismic design codes so as to account for the effects of spatial variation in the seismic design of long-span bridges.

Key words : fragility curve, concrete bridge, nonlinear dynamic analysis, earthquake, ductility

1. Introduction

While performing a seismic risk analysis of highway system, it is imperative to identify seismic vulnerability associated with various damage states of bridges, since the bridges are among the most seismically vulnerable structures in the system. The fragility curve of a bridge, representing its seismic vulnerability, is traditionally defined as the probability that the structure under consideration will suffer from physical damage in a specific state upon subjected to an earthquake ground motion of a given intensity level. In principle, the development of bridge fragility curves requires synergistic use of the following approaches: (1) professional judgment, (2) quasi-static and design code consistent analysis, (3) utilization of damage data associated with past earthquakes and (4) numerical simulation of seismic response based on structural dynamics. More recently, a number of studies on fragility curves for highway bridges were made along these lines.[1]-[6] Most of them, whether empirical or analytical, were based on the assumption that the structure under consideration is subjected to an identical ground motion. However, a majority of multi-span bridges are likely to suffer ground motions at their supports that can differ considerably in amplitude and phases as well as frequency content, since seismic ground motion can vary significantly over distances comparable to the length of the bridge.

The collapse of the 483-meter long bridge at the Interstate 5 and State Road 14(SR14/I5) Interchange located approximately 12 km from the epicenter during the 1994 Northridge earthquake is an example suggesting that the effects of the spatial variation of the ground motion might have caused the failure considering the length of the bridge and the different soil conditions at the locations of the various supports.[7]

* (주)대우건설 토목기술팀, 차장(대표저자 : ksh1210@chol.com)
본 논문에 대한 토의를 2003년 2월 28일까지 학회로 보내 주시면 그 결과를 게재하겠습니다. (논문접수일 : 2003. 8. 25 / 심사종료일 : 2003. 11. 20)

A preliminary investigation was performed earlier by Shinozuka et al[8] on seven typical California bridge models, through which it was found that for several of the bridges the differential support ground motion produces significantly higher structural response than the identical support ground motion. As a result, the assumption of identical support ground motion is unconservative in that peak ductility demand for columns would be underestimated, if the bridge were to be analyzed using identical support ground motion, rather than differential support ground motion. Therefore, it is of paramount importance to account for the effect of spatial variation of earthquake ground motion in developing fragility curves for highway bridges, particularly for multi-span long bridges.

2. Generation of Seismic Ground Motion With Spatial Variation

The spatial variation of seismic ground motion can be attributed to the following three mechanisms[9]-[11] : 1) the difference in arrival times of the seismic waves at different locations, commonly known as the "wave passage effect", 2) the change in shape of the propagating waveform due to multiple scatterings of the seismic waves in the highly inhomogeneous soil medium, referred to as the "incoherence effect", and 3) the change in amplitude and frequency content of ground motion at different locations on the ground surface due to different local soil conditions known as the "local site effect".

In this paper, the computer code has been developed to generate differential acceleration time histories at several prescribed locations on the ground surface. They are compatible with prescribed response(or power) spectra and duration of strong motion, and reflecting the three effects mentioned above.

2.1 Simulation of n-Variate Non-Stationary Stochastic Processes

This section outlines the algorithm which simulates non-stationary ground motion time histories based on a prescribed spectral density matrix. The vector process is assumed to be a non-stationary vector process with evolutionary power. To be specific, consider a n-variate, non-stationary stochastic vector process with components $f_j^0(t);\ j=1,2,\cdots n$, having mean value equal to zero i.e. $\varepsilon[f_j^0(t)]=0;\ i=1,2,\cdots,n$ and cross-spectral density matrix given by:

$$S^0(\omega,t)=\begin{bmatrix} S_{11}^0(\omega,t) & S_{12}^0(\omega,t) & \cdots & S_{1n}^0(\omega,t) \\ S_{21}^0(\omega,t) & & & \vdots \\ \vdots & & \ddots & \vdots \\ S_{n1}^0(\omega,t) & \cdots & \cdots & S_{nn}^0(\omega,t) \end{bmatrix} \quad (1)$$

Due to the assumed non-stationarity of the vector process, the cross-spectral density matrix in Eq. (1) will be a function of both frequency ω and time t. For the purpose of this study, a special case of Eq. (1) is assumed to hold:

$$S_{jj}^0(\omega,t)=|A_j(t)|^2 S_j(\omega)\ ;\ j=1,2,\cdots,n \quad (2)$$

$$S_{jk}^0(\omega,t)=A_j(t)A_k(t)\sqrt{S_j(\omega)S_k(\omega)}\,\Gamma_{jk}(\omega)$$
$$j,k=1,2,\cdots,n\ ;\ j\neq k \quad (3)$$

where $A_j(t);j,k=1,2,\cdots,n$ are the modulating functions of the vector process $f_j^0(t);j=1,2,\cdots,n$ and $S_j(\omega);\ j=1,2,\cdots,n$ are the corresponding(stationary) power spectral density functions. The functions $\Gamma_{jk}(\omega);j,k=1,2,\cdots,n;j\neq k$ are the complex coherence functions describing the correlation relationship between the components of the stationary vector process. They are given by:

$$\Gamma_{jk}(\omega)=\gamma_{jk}(\omega)\exp\left[-i\frac{\omega\xi_{jk}}{\nu}\right];\ j,k=1,2,\cdots,n;j\neq k \quad (4)$$

where $\gamma_{jk}(\omega);j,k=1,2,\cdots,n\ ;\ j\neq k$ are the(stationary) coherence functions between $f_j^0(t)$ and $f_k^0(t)$. $\exp\left[-i\frac{\omega\xi_{jk}}{\nu}\right]$ is the wave propagation term where $\xi_{jk}(\omega)$ is the distance between points j and k, and v is the velocity of wave propagation.

Given the simple structure of Eqs. (2)~(3), where the modulating function is deterministic, the components of the non-stationary process $f_j^0(t);\ j=1,2,\cdots,n$ can be expressed as a product of a zero mean stationary process $g_j^0(t);j=1,2,\cdots,n$ and the respective modulating function, i.e.

$$f_j^0(t)=A_j(t)g_j^0(t);\ j=1,2,\cdots,n \quad (5)$$

$$\varepsilon[g_j^0(t)]=0;\ j=1,2,\cdots,n \quad (6)$$

From Eqs. (2), (3) and (5), the cross-spectral density matrix for the stationary process $g_j^0(t);j=1,2,\cdots,n$ is given by:

$$S^0(\omega)=[\sqrt{S_j(\omega)S_k(\omega)}\,\Gamma_{jk}(\omega)]j,k=1,2,\cdots,n \quad (7)$$

where we have adopted the convention $F_{jj}=1$ and used the notation in Eqs. (2)~(3).

2.2 Simulation Procedure

In order to simulate samples of the n-variate non-stationary stochastic process $f_j^0(t); j=1,2,\cdots,n$, its(stationary) cross-spectral density matrix $S^0(\omega)$ given in Eq. (7) is factorized into the following product:

$$S^0(\omega)=\mathrm{H}(\omega)\mathrm{H}^{T*}(\omega) \tag{8}$$

$$H(\omega,t)\begin{bmatrix} H_{11}(\omega) & & & \\ H_{21}(\omega) & H_{22}(\omega) & & \\ \vdots & \vdots & \ddots & \\ H_{n1}(\omega) & \cdots & \cdots & H_{nn}(\omega) \end{bmatrix} \tag{9}$$

using Cholesky's decomposition method. The diagonal elements of $\mathrm{H}(\omega)$ are real and non-negative functions of ω, while the off-diagonal elements are generally complex functions of ω. The elements of $H(\omega)$ can be written in polar form as:

$$H_{jk}(\omega)=|H_{jk}(\omega)|e^{i\theta_{jk}(\omega)}\ ;\ j>k \tag{10}$$

where:

$$\theta_{jk}(\omega)=\tan^{-1}\left(\frac{\mathrm{Im}[H_{jk}(\omega)]}{\mathrm{Re}[H_{jk}(\omega)]}\right) \tag{11}$$

Once the matrix $S^0(\omega)$ is decomposed according to Eqs. (8)~(10), the stationary stochastic vector process $g_j^0(t); j=1,2,\cdots,n$ can be simulated by the following series as $N\rightarrow\infty$.

$$g_j(t)=2\sum_{m=1}^{n}\sum_{l=1}^{N}|H_{jm}(\omega_l)|\sqrt{\Delta\omega}\cos[\omega_l t-\theta_{jm}(\omega_l)+\Phi_{ml}];\ j=1,2,\cdots,n \tag{12}$$

where

$$\omega_l=1\Delta\omega\ ;\ l=1,2,\cdots,N \tag{13}$$

$$\Delta\omega=\frac{\omega_u}{N} \tag{14}$$

$$\theta_{jm}(\omega_l)=\tan^{-1}\left(\frac{\mathrm{Im}[H_{jm}(\omega_l)]}{\mathrm{Re}[H_{jm}(\omega_l)]}\right) \tag{15}$$

The quantities $\{\Phi_{ml}\}; m=1,2,\cdots,n; l=1,2,\cdots,N$ appear ing in Eq. (12) are n sequences of independent random phase angles distributed uniformly over the interval $[0,2\pi]$. In Eq. (14), ω_u represents an upper cut-off frequency beyond which the elements of the cross-spectral density matrix in Eq. (1) may be assumed to be zero for any time instant t. As such, ω_u is a fixed value and hence $\Delta\omega\rightarrow 0$ as $N\rightarrow\infty$, so that $N\Delta\omega=\omega_u$.

In order to generate the i-th sample $g_j^{(i)}(t); j=1,2,\cdots,n$ of the stationary stochastic vector process $g_j(t); j=1,2,\cdots,n$, one replaces the n sequences of random phase angles $\{\Phi_{ml}\}; m=1,2,\cdots,n; l=1,2,\cdots,N$ in Eq. (12) with their respective i-th realizations $\{\Phi_{ml}\}; m=1,2,\cdots,n; l=1,2,\cdots,N$:

$$g_j^{(i)}(t)=2\sum_{m=1}^{n}\sum_{l=1}^{N}|H_{jm}(\omega_l)|\sqrt{\Delta\omega}\cos[\omega_l t-\theta_{jm}(\omega_l)+\Phi_{ml}^{(i)}];\ j=1,2,\cdots,n \tag{16}$$

The corresponding i-th realization of the non-stationary vector process $f_j^{(i)}(t); j=1,2,\cdots,n$ is calculated by multiplying the i-th realization of the stationary process $g_j^{(i)}; j=1,2,\cdots,n$ by the modulating functions $A_j(t); j=1,2,\cdots,n$:

$$f_j^{(i)}(t)=A_j(t)g_j^{(i)};\ j=1,2,\cdots,n \tag{17}$$

2.3 Simulation of Ground Motion Compatible with Prescribed Response Spectra

An iterative algorithm shown in Table 1 is used to generate acceleration time histories at n points on the ground surface that are compatible with prescribed response spectra. A different target acceleration response spectrum $RSA_i(\omega); i=1,2,\cdots,n$ can be assigned to each of these points, since those points can generally be on different local soil conditions. Complex coherence functions $\Gamma_{jk}(\omega); j,k=1,2,\cdots,n; j\neq k$ are prescribed between pairs of points and modulating functions $A_j(t); j=1,2,\cdots,n$ are assigned at each point. The power spectral density functions $S_j(\omega); j=1,2,\cdots,n$ in the first iteration are initialized to a constant (non-zero) value over the entire frequency range. After setting up the cross-spectral density matrix given in Eq. (7) according to a prescribed coherence function and a velocity of wave propagation, the stationary ground motion time histories are generated using the simulation formula given in Eq. (12). The non-stationarity is then introduced by multiplying each of the stationary time histories with modulating functions $A_j(t); j=1,2,\cdots,n$. In the next step, the response spectra of the simulated non-stationary time histories are calculated and matched with the prescribed response spectra. In case, the response spectra do not match at a chosen level of accuracy, the diagonal terms of the cross-spectral density matrix of the underlying stationary are upgraded as shown in Table 1.

Asynchronous acceleration and displacement time histories at three different locations were shown in Fig. 1 & 2 respectively.

Table 1 Iterative Scheme to Generate Acceleration Time Histories Compatible Response Spectrum at n Points on the Ground Surface

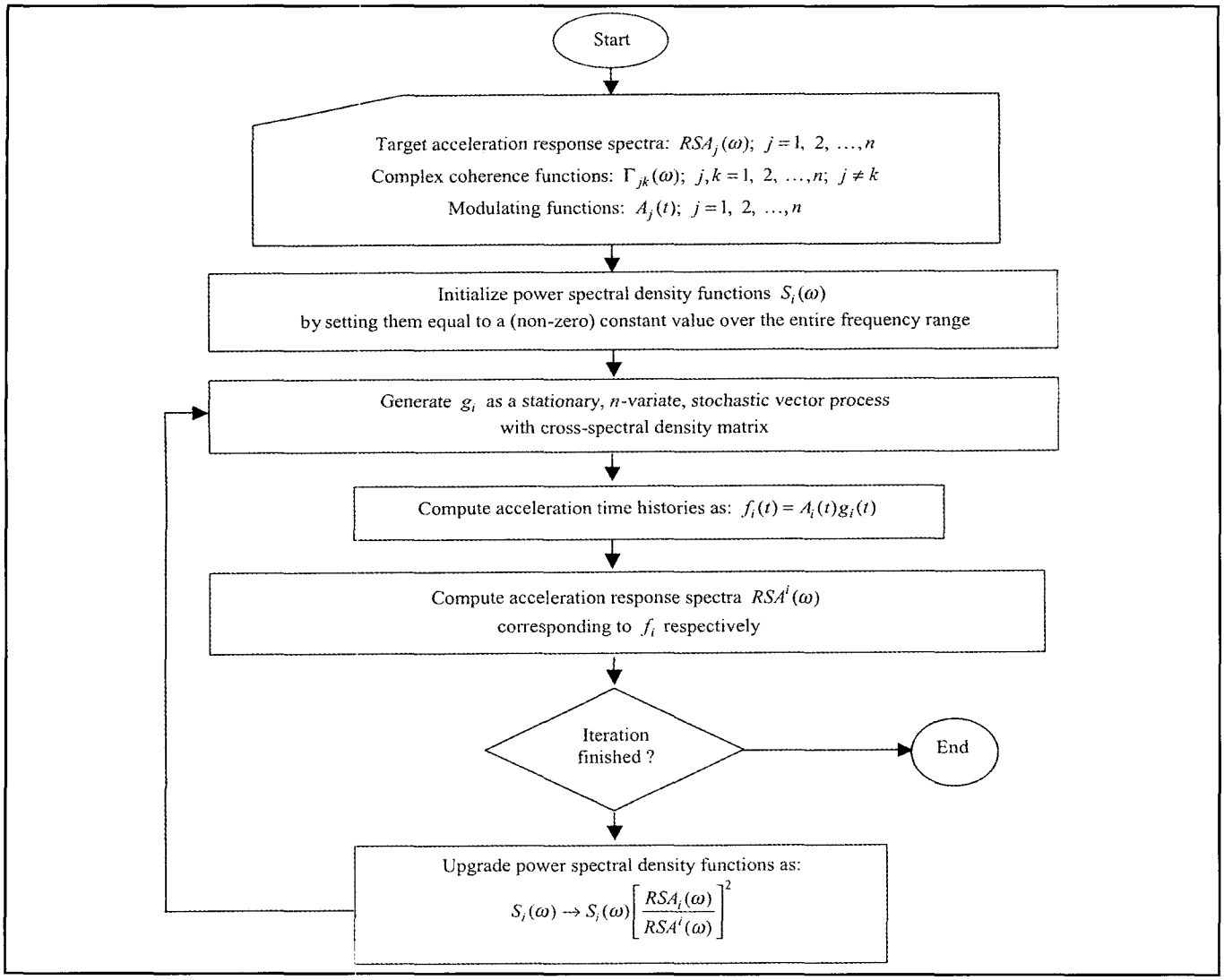

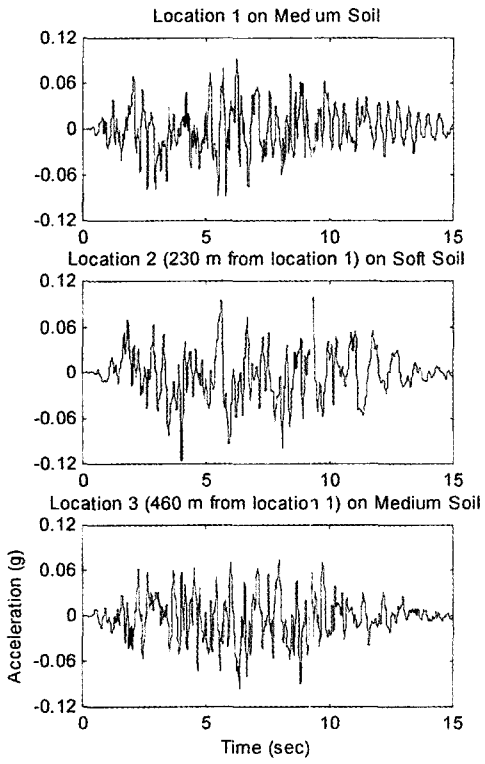

Fig. 1 Acceleration Time Histories

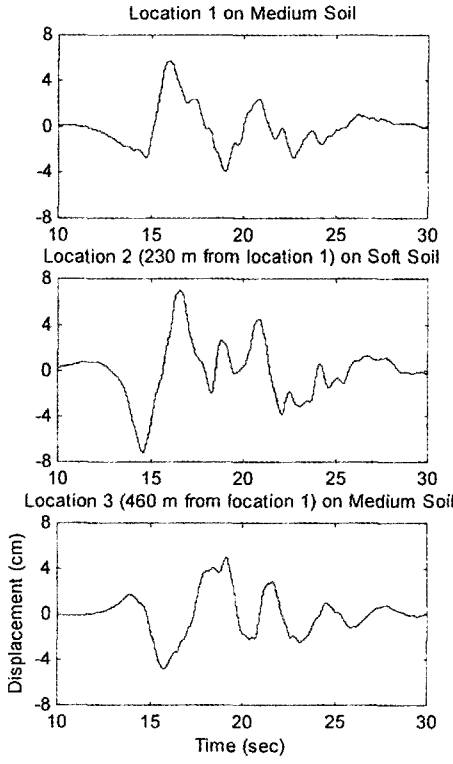

Fig. 2 Displacement Time Histories

3. Bridge Models

Two actual concrete bridges(SR14/I5 Interchange & Santa Clara Bridge) in California are selected for this study. The geometry and boundary conditions for these bridges are shown in Fig. 3. The overall length of SR14/I5 Interchange built with four hinges is 483 meter and the nine columns have different heights from 9.5 meter up to 34.4 meter, while that of Santa Clara Bridge built with one hinge is 500 meter and each one of the eleven columns has a height of 12.8 meter.

The nonlinearities included in this study are yielding of columns and pounding of decks at the expansion joint.[12] The plastic hinge formed in the bridge column is assumed to have bilinear hysterestic characteristics. The expansion joint is constrained in the relative vertical movement, while freely allowing horizontal opening movement and rotation. The closure at the joint, however, is restricted by a gap element when the relative motion of adjacent decks exhausts the initial gap width of 2.54cm(1.0 in). The bases of the columns were assumed to be fixed, while the two abutments were modeled as roller supports. To reflect the cracked state of a concrete bridge column for the seismic response analysis, an effective moment of inertia is employed, making the period of the bridge longer. The Column Ductility Program *COLx*[13] is used to model the moment-curvature relationship of plastic hinges for columns. The parameter used to describe the nonlinear structural response in this study is the ductility demand. The ductility demand is defined as θ/θ_y, where θ is the rotation of a bridge column in its plastic hinge and θ_y is the corresponding rotation at the yield point. The nonlinearities involved in the bridge analytical model are depicted in Fig. 4. The SAP2000/Nonlinear finite element computer code[14] is utilized for the extensive two-dimensional response analysis of the bridge including the nonlinearities.

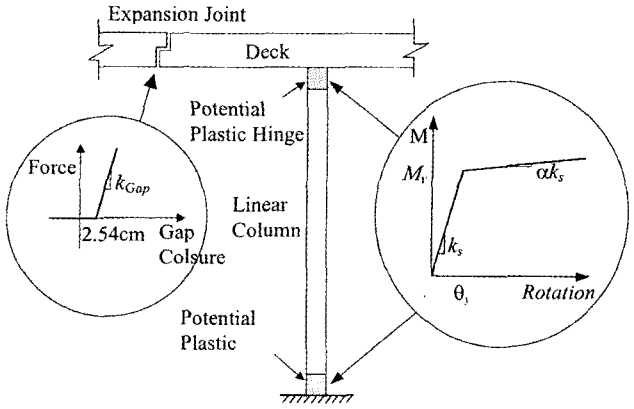

Fig. 4 Nonlinear Model for Bridge Column

4. Development of Fragility Curves

4.1 Fragility Curves

By making use of Monte Carlo simulation techniques, a total of 300 earthquakes without and with spatial variation were generated at the nine supports of SR14/I5 Interchange and at the eleven supports of Santa Clara Bridge. For each set of differential support ground motion time histories, the corresponding set of identical support ground motion time histories is obtained by considering that the ground motion time history at the first support of the bridge is applied at all the other supports. The computer code SAP2000/Nonlinear was utilized in order to simulate the state of damage of the structure under ground displacement time histories without and with spatial variation.

In order to incorporate various structural characteristics that affect damage into fragility analysis, some definitions according to failure mechanisms resulting in different damage states are investigated. For the ease of demonstration, however, the five states of damage considered for the bridges in this study are light(at least one column subjected to ductility demand $\rho \geq 1$), minor(at least one column subjected to ductility demand $\rho \geq 2$), moderate(at least one column

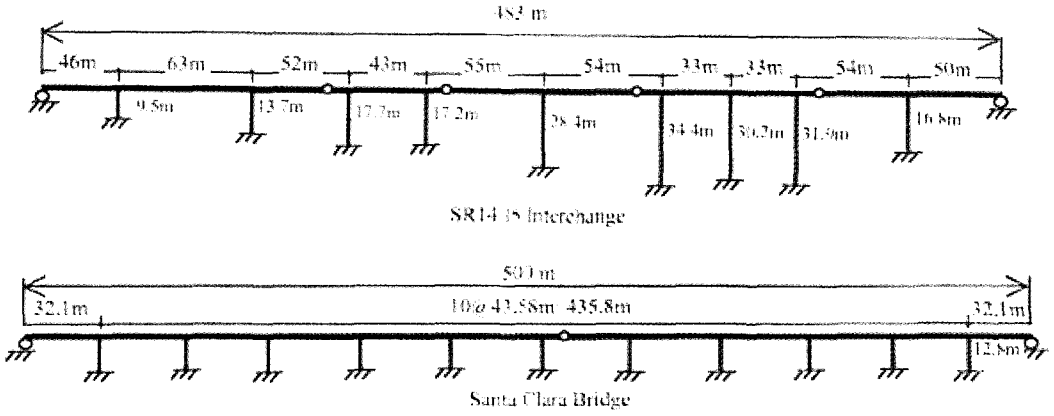

Fig. 3 Elevation of Two Bridges

subjected to ductility demand $\rho \geq 3$), major(at least one column subjected to ductility demand $\rho \geq 4$) and collapse (at least one column subjected to ductility demand $\rho \geq 5$) under the longitudinal applications of ground motion.

A common log-standard deviation, which forces the fragility curves not to intersect, is estimated along with the medians of the lognormal distributions with the aid of the maximum likelihood method. The following likelihood formulation described by Shinozuka et al[3),(4)] is introduced for the purpose of this method. Although this method can be used for any number of damage states, it is assumed here for the explanation of analytical procedure that there are four states of damage including the state of no damage. A family of three (3) fragility curves exists in this case where events E_1, E_2, E_3 and E_4 respectively indicate the state of no, at least minor, at least moderate and major damage. $P_{ik}=P(a_i, E_k)$ in turn indicates the probability that a bridge i selected randomly from the sample will be in the damage state E_k when subjected to ground motion intensity expressed by PGA=a_i. All fragility curves are represented by two-parameter lognormal distribution functions

$$F_j(a_j;' c_j, \zeta_j) = \Phi\left[\frac{\ln(a_i/c_j)}{\zeta_j}\right] \tag{18}$$

where c_j and ζ_j are the median and log-standard deviation of the fragility curves for the damage state of "at least minor", "at least moderate" and "major" identified by j= 1, 2 and 3. From this definition of fragility curves, and under the assumption that the log-standard deviation is equal to ζ common to all the fragility curves, one obtains;

$$P_{i1} = P(a_i, E_1) = 1 - F_1(a_i; c_1, \zeta) \tag{19}$$

$$P_{i2} = P(a_i, E_2) = F_1(a_i; c_1, \zeta) - F_2(a_i; c_1, \zeta) \tag{20}$$

$$P_{i3} = P(a_i, E_3) = F_3(a_i; c_2, \zeta) - F_2(a_i; c_3, \zeta) \tag{21}$$

$$P_{i4} = P(a_i, E_4) = F_3(a_i; c_3, \zeta) \tag{22}$$

The likelihood function can then be introduced as

$$L(c_1, c_2, c_3, \zeta) = \prod_{i=1}^{n} \prod_{k=1}^{4} P_k(a_i; E_k)^{x_{ik}} \tag{23}$$

where

$$x_{ik} = 1 \tag{24}$$

if the damage state E_k occurs the i-th bridge subjected to $a = a_i$, and

$$x_{ik} = 0 \tag{25}$$

otherwise. Then the maximum likelihood estimates c_{oj} for c_j and ζ_o o for ζ are obtained by solving the following equations,

$$\frac{\partial \ln L(c_1, c_2, c_3, \zeta)}{\partial c_j} = \frac{\partial \ln L(c_1, c_2, c_3, \zeta)}{\partial \zeta} = 0 \quad (j = 1, 2, 3) \tag{26}$$

by implementing a straightforward optimization algorithm.

The fragility curves for the longitudinal direction of SR14/I5 Interchange associated with these states of damage were plotted in Fig. 5(a) for the case 1 "without spatial variation and without pounding", in Fig. 5(b) for the case 2 "with spatial variation and without pounding", in Fig. 5(c) for the case 3 "without spatial variation and with pounding" and in Fig. 5(d) for the case 4 "with spatial variation and with pounding" as a functions of different measures of ground motion intensity including PGA, PGV, SA, SV and SI, in order to compare and highlight how ground motions with spatial variation and/or pounding affect structural behavior. The fragility curves for Santa Clara Bridge were also plotted in Figs. 6(a), 6(b), 6(c) and 6(d) in the same way.

It should be noted that the values of the ground motion intensity such as PGA, PGV, SA, SV and SI are different at different supports of the bridge for the case with spatial variation. For the purpose of practicality, these values are averaged and noted as Mean PGA, Mean PGV, Mean SA, Mean SV and Mean SI in Figs. 5(b) and 5(d), and in Figs. 6(b) and 6(d). The distribution of values of measures of ground motion intensity is plotted in Fig 7. Since the generated ground motion time histories are more compatible with the prescribed PGA values than the others, it is expected that the fragility curve as the function of PGA might be the best fit for the purpose of comparison in this study.

4.2 Measures of Ground Motion Intensity

Expressing the fragility curves as functions of different measures of ground motion intensity has been advocated and promoted by many researchers and engineers. PGA, which is the absolute maximum value of the ground acceleration associated with a particular ground acceleration time history, has been most often used to represent the

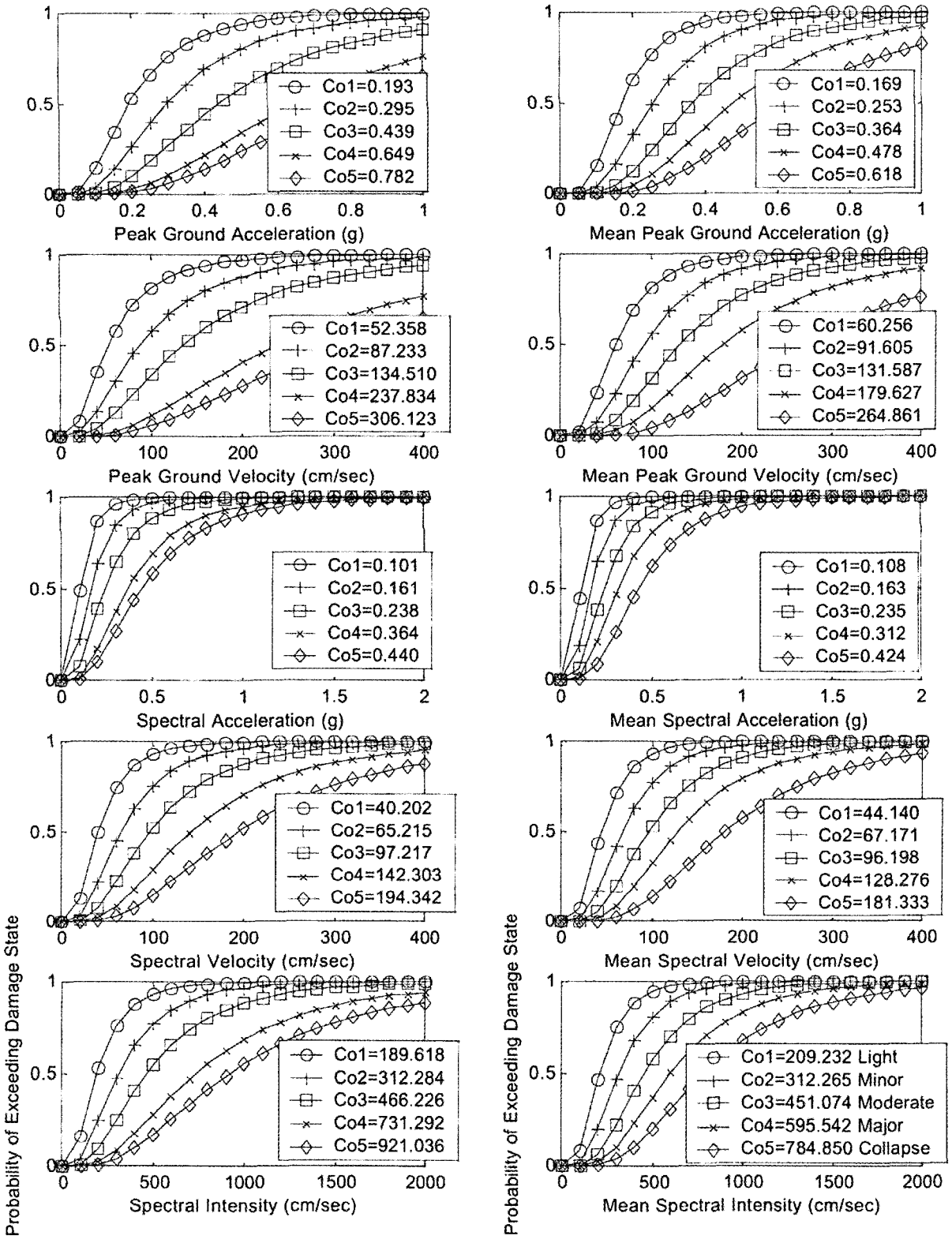

(a) Case 1(without spatial variation and without pounding)

(b) Case 2(with spatial variation and without pounding)

Fig. 5 Fragility curves for SR14/I5 Interchange

ground motion intensity for fragility curve development. However, SA, the maximum pseudo response acceleration of a damped single-degree-of-freedom system to the ground acceleration, is also prominent among these alternative measures. Indeed, SA can be a good measure when the structural response is primarily in the linear range, structural dynamic characteristics including damping properties are reasonably well known, geotechnically consistent earthquake ground motion time histories are either easily specificable or readily available from pertinent database, and the state of damage for which the fragility curve is to be developed depends mainly on the instantaneous maximum inertia

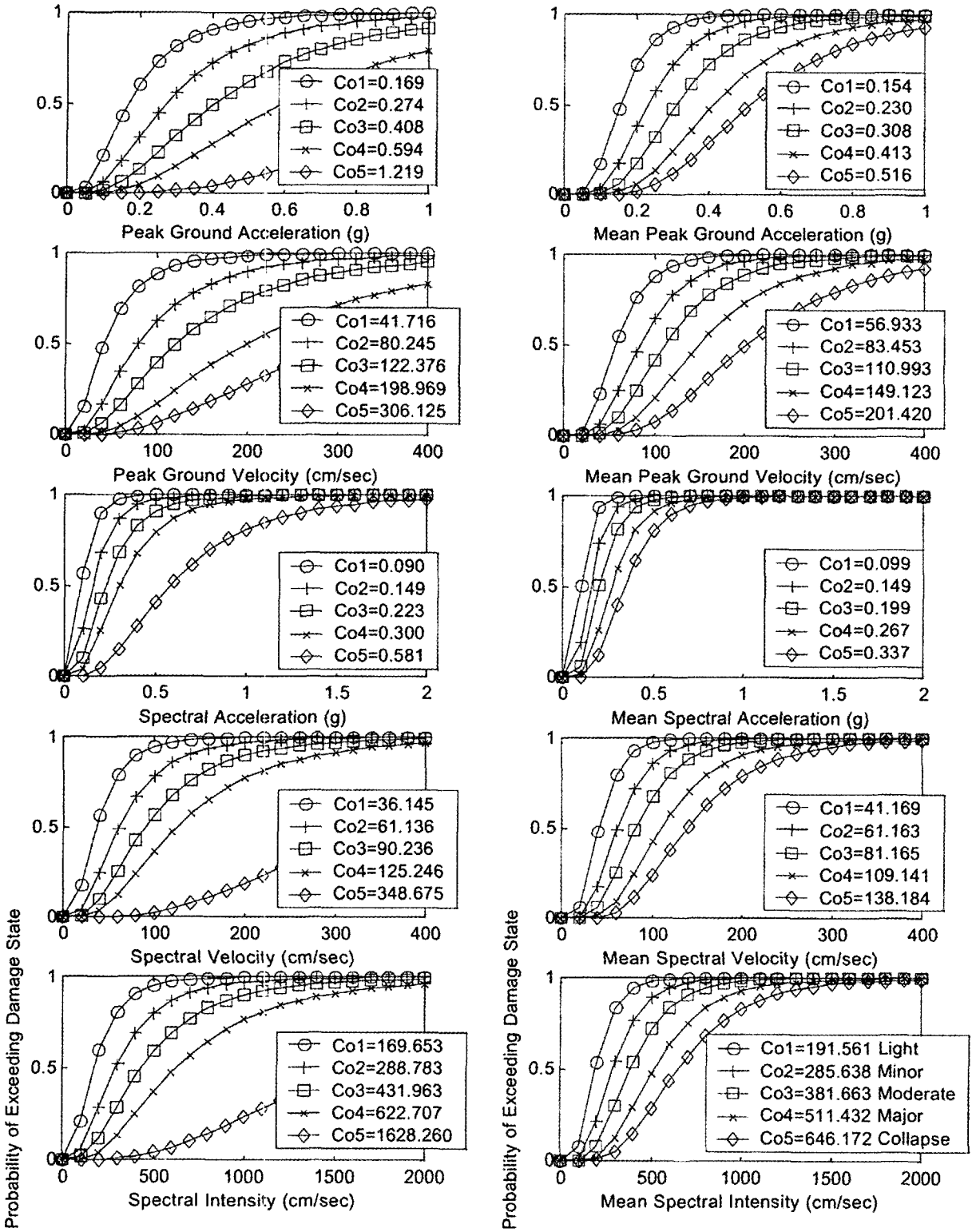

(c) Case 3(without spatial variation and with pounding)

(d) Case 4(with spatial variation and with pounding)

Fig. 5 Fragility curves for SR14/I5 Interchange

force exerted by a ground motion time history.

Some researchers also claim that ground velocity-related quantities including PGV, SV and SI are more appropriate for this purpose. PGV is the absolute maximum value of the ground velocity associated with a particular ground velocity time history, SV is the maximum pseudo response velocity of a damped single-degree-of-freedom system to the ground acceleration, and SI is the average of SV over the natural period between 0.1 and 2.5 sec following the original Housner's definition.[15] The structural damping coefficient is assumed in all calculations to be 5%, although Housner used 2% for SI calculations.

4.3 Effect of Spatial Variation

If the bridge damage is more susceptible to the ground motion with spatial variation than without it, the simulated fragility curves are at least consistent with the hypothesis that, for all levels of damage state, the median fragility values without spatial variation are larger than the corresponding values with spatial variation. The hypothesis is perfectly satisfied, however, only when the comparisons are made on the basis of the median ground motion intensity values measured in PGA for the cases of Figs 5(a) and 5(b), and Figs 6(a) and 6(b). Other measures such as PGV, SA, SV

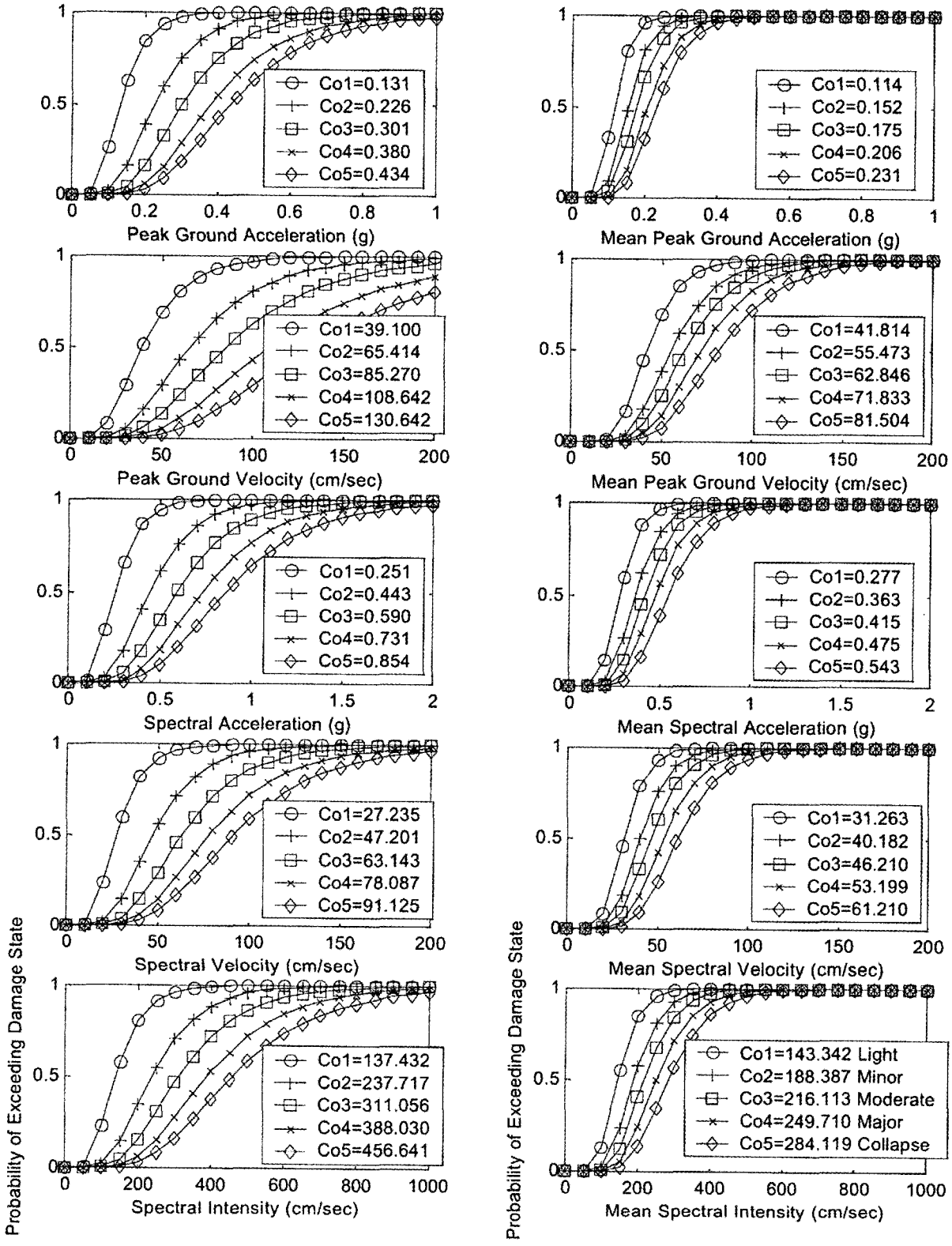

(a) Case 1(without spatial variation and without pounding)

(b) Case 2(with spatial variation and without pounding)

Fig. 6 Fragility curves for Santa Clara Bridge

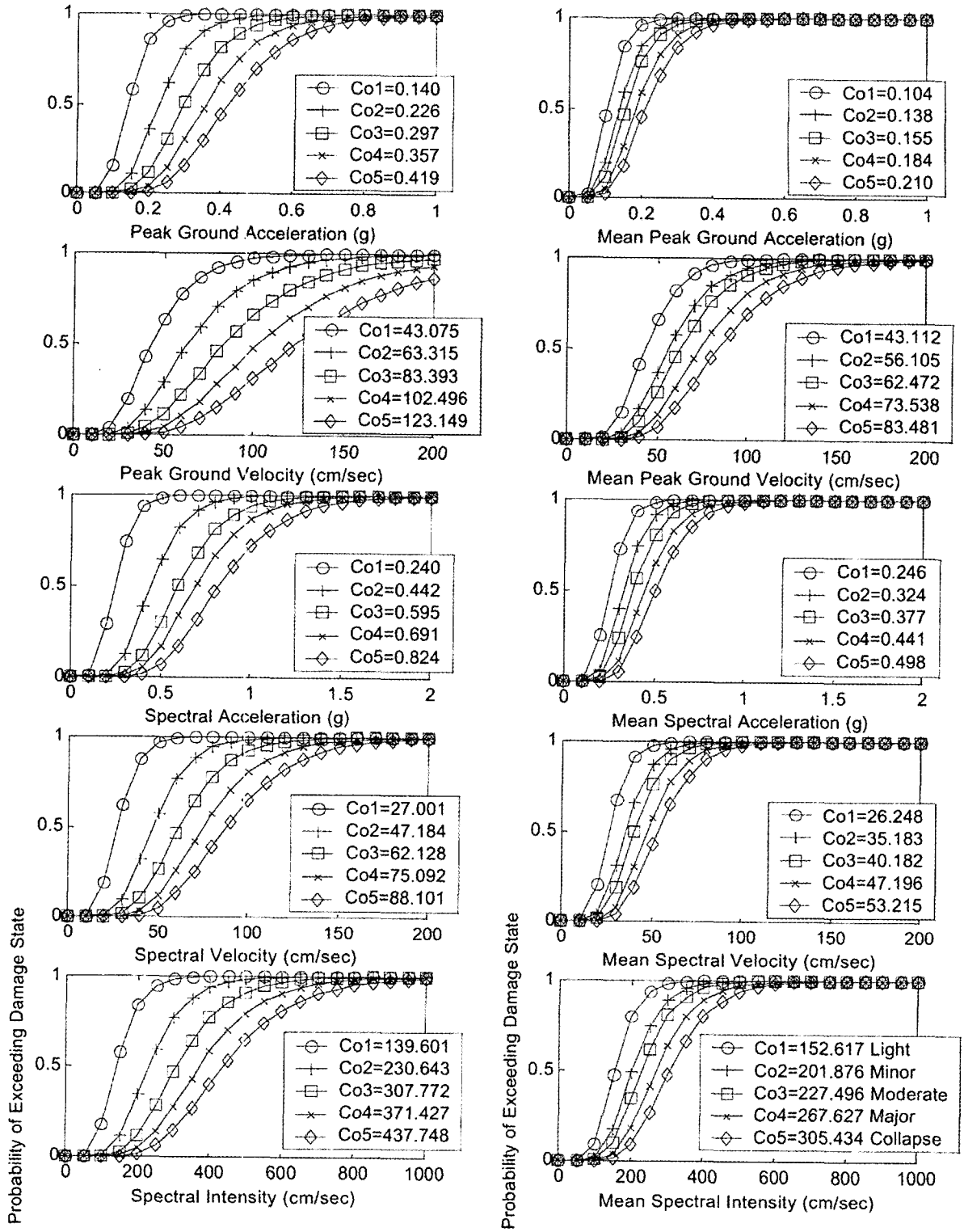

(c) Case 3(without spatial variation and with pounding) (d) Case 4(with spatial variation and with pounding)

Fig. 6 Fragility curves for Santa Clara Bridge

and SI produce mixed results in such a way that spatial variation is detrimental only for severer states of damage, while it appears even beneficial for lighter states of damage. However, this observation may be superfluous. Since when ground motion time histories are simulated, only their peak ground accelerations are targeted.

In particular, if the number of bridges at a certain state of damage(e.g., at least light damage) is counted, it is larger when the entire sample is subjected to the ground motion with spatial variation than without it. In fact, the percentage of bridges subjected to the specific damage state for the longitudinal directions of SR14/I5 Interchange and Santa Clara Bridge under ground motion for the case1, 2, 3 and 4 was listed in Table 2. Examining Table 2,

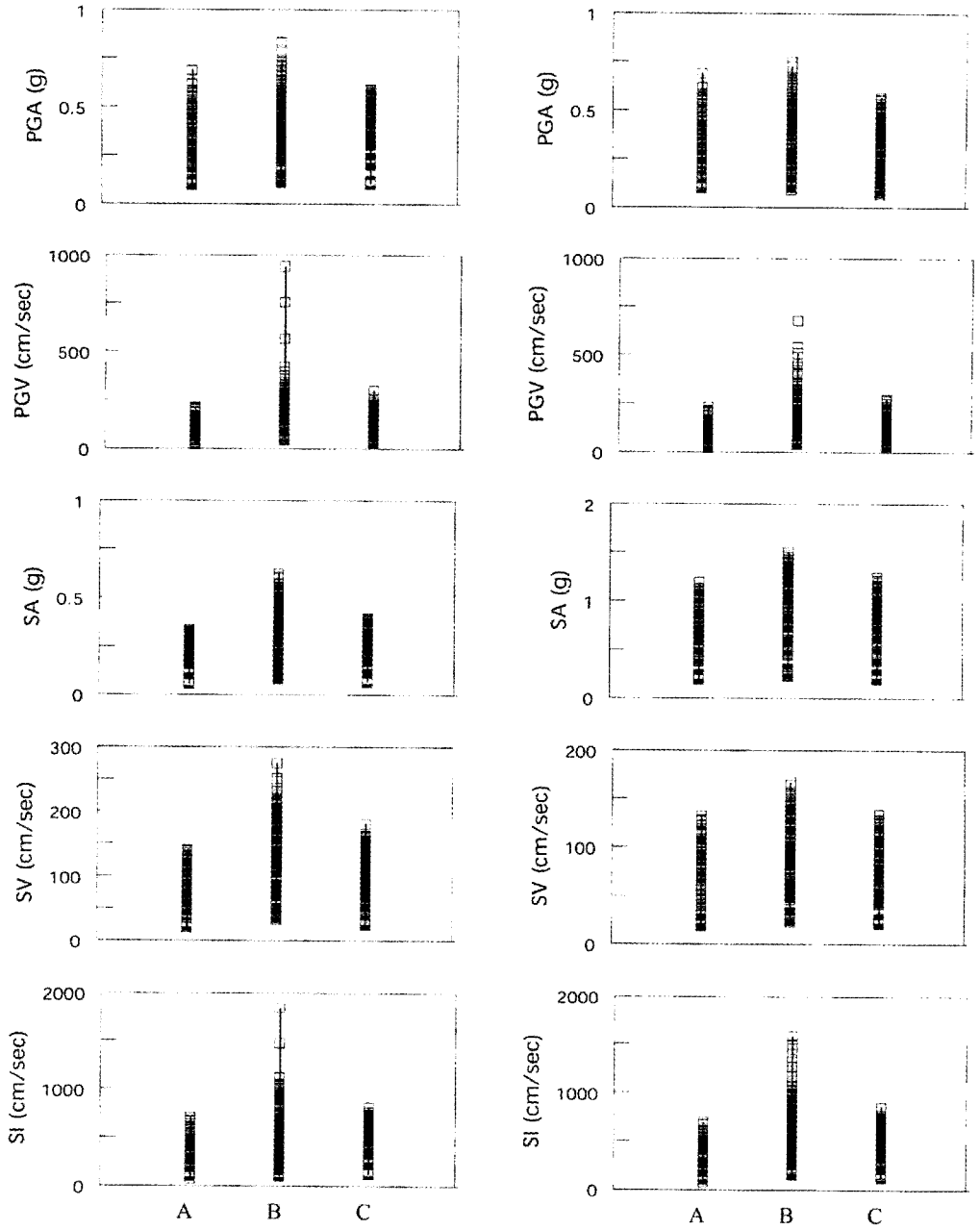

Fig. 7 Distribution of values of measures of ground motion intensity(sample size=300)

Table 2 Percentage of Damaged Bridges(sample size=300)

	SR14/I5 Interchange				Santa Clara Bridge			
Damage State	Case 1	Case 2	Case 3	Case 4	Case 1	Case 2	Case 3	Case 4
Light	76	79	79	80	84	88	80	86
Minor	54	63	58	67	67	81	68	79
Moderate	29	42	33	53	54	77	55	76
Major	9	22	12	34	40	73	43	70
Collapse	2	7	2	16	29	68	32	64

it is found that the number of damaged bridges increases up to 8 times when the SR14/I5 Interchange is analyzed considering spatial variation and pounding, compared to that without spatial variation and pounding. It is also observed from Table 2 that pounding for the case 3 does not increase the ductility demand(or the number of damaged bridges) very much. Because it is highly unlikely that pounding will take place at the instant of the peak rotation of the column end in such a way that it will further amplify the rotation. Since the SR14/I5 Interchange, however, has four hinges, it has more chances to amplify the rotation increasing the number of damaged bridges rather than the

Santa Clara Bridge does. This observation might not always apply, depending on the details of specific bridge characteristics.

It is noted that if the ground motion time history can be generated for a specific value of PGV, SA, SV and SI, the fragility curves expressed by these ground motion intensities might be a good way to provide useful information related to the structural characteristics of a bridge system. Further research is needed in this respect.

5. Conclusions

This paper presents fragility analysis of two actual bridges under ground motion with spatial variation. The analytical fragility curve is constructed for SR14/I5 Interchange and Santa Clara Bridge utilizing nonlinear dynamic analysis to investigate the effect of spatial variation and/or pounding. Two-parameter lognormal distribution functions are used to represent the fragility curves utilizing the maximum likelihood procedure with each event of bridge damage treated as a realization from a multi-outcome Bernoulli type experiment. In addition, some preliminary evaluations are made on the significance of the fragility curves developed as a function of ground motion intensity measures other than PGA.

The computed fragility curves corresponding to these damage states appear to make intuitive sense relative to the bridge's design, construction, and performance in past seismic events. The following conclusions can be made on the results of this study.

(1) The simulated fragility curves obtained in this study are perfectly consistent with the hypothesis that the bridge is more vulnerable to the ground motion with spatial variation for all levels of damage state only when the comparisons are made on the basis of median ground motion intensity values measured in PGA. PGV, SA, SV and SI showed mixed results, while they are consistent in trend.

(2) For multi-span long bridges subjected to strong ground motion, the effect of spatial variation(and/or pounding) might increase the number of damaged bridges by a significant factor as much as 8 times in this study for the major and collapse damage state where nonlinear effects obviously play a crucial role. Thus, a need is felt to take spatial variation(and/or pounding) into consideration for designing highway bridges.

(3) For the Santa Clara Bridge with an expansion joint, the pounding does not always adversely affect on the column responses, while for the SR14/I5 Interchange with four hinges, it does especially for severer states of damage. However, this observation might not always apply, depending on the details of specific bridge characteristic.

References

1. Basoz, N., and Kiremidjian, A. S., "Evaluation of bridge damage data from the Loma Prieta and Northridge, California earthquake," *Technical Report MCEER-98-0004*, 1998.
2. Hwang, H., Jernigan, J. B., and Lin, Y. W., "Expected seismic damage to Memphis highway systems," *Proceeding of 5th U.S. Conference on Lifeline Earthquake Engineering*, 1999.
3. Shinozuka, M., Feng, M. Q., Kim, H.-K., Uzawa, T., and Ueda, T., "Statistical analysis of fragility curves," *Technical Report MCEER*, 2000a.
4. Shinozuka, M., Uzawa, T., and Sheng, L.-H., "Estimation and testing of fragility parameters," International Conference on Monte Carlo Simulation, 2000b.
5. Shinozuka, M., Feng, M. Q., Lee, J., and Nagaruma, T., "Statistical analysis of fragility curves," *J. Engrg. Mech.* ASCE, Vol. 126, No. 12, 2000c, pp. 1224-1231.
6. Shinozuka, M., Feng, M. Q., Kim, H.-K., and Kim, S.-H., "Nonlinear static procedure for fragility curve development," *J. Engrg. Mech.* ASCE, Vol. 126, No. 12, 2000d, pp. 1287-1295.
7. Buckle, I. G.(Editor), "The Northridge, California Earthquake of January 17, 1994: Performance of Highway Bridge," *Technical Report NCEER-94-0008*, National Center for Earthquake Engineering Research, State University of New York, Buffalo, 1994.
8. Shinozuka, M., Deodatis, G., Saxena, V., Kim, H.-K., "Effect of spatial variation of ground motion on bridge response," *Technical Report MCEER*, 1998.
9. Deodatis, G., *Simulation of stochastic processes and fields to model loading and material uncertainties: Probabilistic methods for structural design*, Kluwer Academic Publshers, 1996a.
10. Deodatis, G., "Simulation of ergodic multi-variate stochastic processes," *J. Engrg. Mech.*, ASCE, Vol. 122, No. 8, 1996b, pp. 778-787.
11. Deodatis, G., "Non-stationary stochastic vector processes: Seismic ground motion applications," *Probabilistic Engrg. Mech.*, Vol. 11, No. 3, 1996c, pp. 149-167.
12. Kim, S.-H. and Shinozuka, M., "Effects of seismically inducd pounding at expansion joints of concrete bridges," *J. Engrg. Mech.* ASCE, Vol. 129, No. 11, 2003.
13. California Department of Transportation, *COLx Users*

Manual, Sacramento, CA, 1993.

14. Computer and Structures, Inc., *SAP2000/Nonlinear Users Manual*, Berkeley, CA, 1999.
15. Hausner, G. W., "Intensity of ground motion during strong earthquakes," *Proceedings of 1952 Symposium on Earthquake and Blast Effects on Structures*, Earthquake Engineering Research Institute, California Institute of Technology, 1952.